

A NOVEL SCHEME BASED ON ANGULAR DISPERSION-INDUCED MICROBUNCHING MECHANISM FOR HARMONIC GENERATION IN STORAGE RING*

Yujie Lu, ShanghaiTech University, 201210 Shanghai, China

Chao Feng¹, Dong Wang, Shanghai Advanced Research Institute, Chinese Academy of Sciences, 201210 Shanghai, China

¹also at University of Chinese Academy of Sciences, 101408 Beijing, China

Abstract

Angular dispersion-induced microbunching (ADM) scheme was proposed to generate high harmonic coherent radiation in the storage ring with weak energy modulation amplitude. However, it is still difficult to convert the external UV seed laser into the sub-nanometer wavelength. In this paper, we proposed a novel scheme based on ADM mechanism. By properly choosing the parameters, theory and one order simulation demonstrate that it is possible to produce ultrahigh harmonic coherent radiation in the storage ring. The high harmonic conversion efficiency of the proposed scheme may open up a new opportunity to produce sub-nanometer X-ray coherent radiation in the storage ring.

INTRODUCTION

Free electron laser (FEL) based on linear accelerator and synchrotron radiation based on electron storage ring are two kind of large-scale light source facilities in the world which have wide application in multiple disciplines research including physics, chemistry, material science and so on.

Self-seeding [1, 2] and X-ray FEL oscillator (XFELO) schemes [3–5] are proposed in the field of FEL to generate the fully coherent radiation with ultrashort wavelength. Besides, several schemes based on external seeding FEL are proposed to improve the longitudinal coherence and harmonic conversion efficiency. Among these harmonic conversion schemes based on external seeding FEL, echo-enabled harmonic generation (EEHG) [6] was proposed to convert a UV seed laser into the shorter wavelength at the water window region in a single stage. However, limited by the beam characteristics (low current and large energy spread) in the storage ring, the seed laser with high peak power is needed which will result in a larger beam energy spread. It will affect the final radiation process. In addition, it is still difficult to extend the radiation wavelength to below 1 nm driven by a UV seed laser. Taking advantage of the low vertical emittance in the storage ring, angular dispersion-induced microbunching (ADM) scheme [7] was proposed to generate high harmonic coherent radiation with weak energy modulation amplitude. Borrowing the idea of triple modulator-chicane (TMC) scheme [8], we propose a novel

scheme based on the ADM, for generating sub-nanometer wavelength coherent radiation. The high harmonic conversion efficiency of the proposed scheme has potential to allow the generation of the fully coherent radiation at the sub-nanometer wavelength in the storage ring.

METHODS

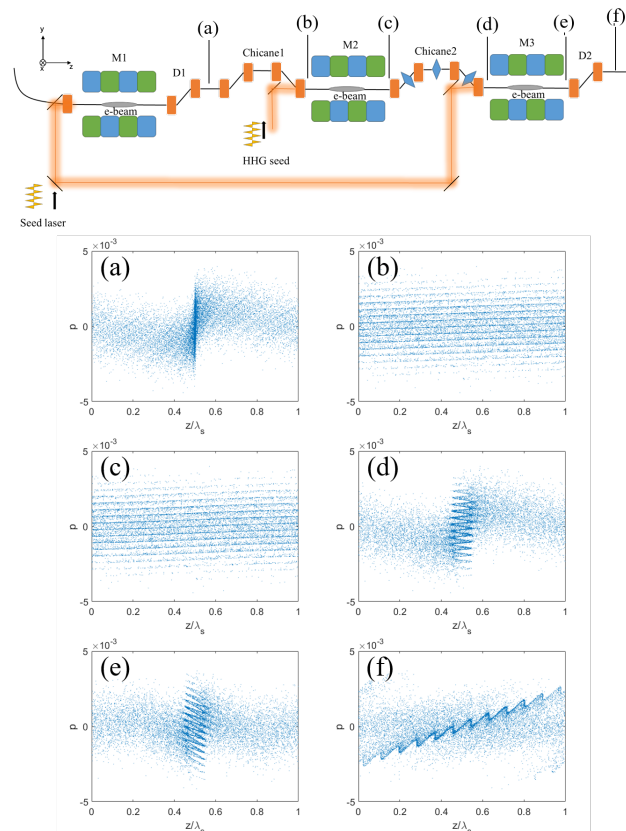


Figure 1: Schematic layout of the proposed scheme based on ADM mechanism.

The schematic layout of the proposed scheme based on the ADM mechanism is shown in Fig. 1. The electron beam from storage ring will firstly go through the ADM mechanism which consists of one bend magnet, a modulator (M1) and a dogleg (D1). Then the beam will be sent to the first chicane, the second modulator (M2), the second chicane, the third modulator (M3) and the second dogleg (D2). Here we assume that the lasers in M1 and M3 have the same

* WORK SUPPORTED BY THE NATIONAL NATURAL SCIENCE FOUNDATION OF CHINA (11975300, 12122514) AND SHANGHAI SCIENCE AND TECHNOLOGY COMMITTEE RISING-STAR PROGRAM, CHINA (20QA1410100).

wavelength, but π phase difference, and the first chicane and the second chicane have the opposite momentum compact factor.

Following the analysis in Ref. [6], we assume that the bunch length is much larger than the wavelength of the lasers. Therefore, we can define that the initial longitudinal distribution of a longitudinally uniform beam can be expressed as: $f_0(Y'_0, P_0) = N_0(2\pi)^{-1}e^{-P_0^2/2}e^{-Y_0'^2/2}$, where N_0 is the number of electrons per unit length of the beam, $Y'_0 = \frac{y'_0}{\sigma_{y'}}$ is the normalized vertical beam divergence coordinate, y'_0 is the initial beam divergence coordinate, $\sigma_{y'}$ is initial beam vertical divergence, $P_0 = (E - E_0)/\sigma_E$ is the dimensionless energy deviation, E_0 is the average electron energy, σ_E is the RMS energy spread. The laser phase as experienced by the electron bunch is given by $\xi_0 = k_1 z_0$, where k_1 is the wavenumber of the seed laser in M1 and z_0 the initial beam longitudinal coordinate. The wave number of the seed laser in M1 can be expressed as k_1 . The modulation process of the ADM mechanism can be respectively written as:

$$Y'_1 = Y'_0 + T_1 P_0, \quad (1)$$

$$P_1 = P_0 + A_1 \sin(\xi_0), \quad (2)$$

$$\xi_1 = \xi_0 + C_1 Y'_1 + B_1 P_1, \quad (3)$$

where $T_1 = t\sigma_E/(\sigma_y E_0)$ (t is the first bend magnet angle), $A_1 = \Delta E_1/\sigma_E$ (ΔE_1 is the energy modulation amplitude produced by the first modulator), $B_1 = R_{56}^{(1)} k_1 \sigma_E / E_0$ ($R_{56}^{(1)}$ is the momentum compact factor of the first dogleg), $C_1 = \eta k_1 \sigma_{y'}$ (η is the dispersion strength of the first dogleg). When the beam goes through the first chicane, the second modulator, the second chicane, the third modulator and the final dogleg, the modulation process can be written as:

$$\xi_2 = \xi_1 + B_2 P_1, \quad (4)$$

$$P_2 = P_1 + A_2 \sin(K\xi_2 + \phi), \quad (5)$$

$$\xi_3 = \xi_2 + B_3 P_2, \quad (6)$$

$$P_3 = P_2 + A_3 \sin(\xi_3 + \pi), \quad (7)$$

$$\xi_4 = \xi_3 + C_2 Y'_1 + B_4 P_3, \quad (8)$$

where $B_2 = R_{56}^{(2)} k_1 \sigma_E / E_0$ ($R_{56}^{(2)}$ is the momentum compact factor of the first chicane), $A_2 = \Delta E_2/\sigma_E$ (ΔE_2 is the energy modulation amplitude produced by the second modulator), $K = k_2/k_1$, $B_3 = R_{56}^{(3)} k_1 \sigma_E / E_0$ ($R_{56}^{(3)}$ is the momentum compact factor of the second chicane), $A_3 = \Delta E_3/\sigma_E$ (ΔE_3 is the energy modulation amplitude produced by the third modulator), $C_2 = \eta' k_1 \sigma_{y'}$ (η' is the dispersion strength of the final dogleg), $B_4 = R_{56}^{(4)} k_1 \sigma_E / E_0$ ($R_{56}^{(4)}$ is the momentum compact factor of the second chicane). Here we assume the phase shift between the first laser and third laser in the modulator is π . Therefore, the beam density N as a function of ξ can be expressed as $N(\xi) = \int_{-\infty}^{\infty} dp dY' f_f(\xi, p, Y')$. Therefore, the bunching factor b can be expressed as $b = \frac{1}{N_0} |\langle e^{-i\alpha\xi} N(\xi) \rangle|$. Only if $\alpha = n + mK$, the bunching factor

is non-zero, where n and m are integers. After some mathematical manipulation, the bunching factor can be expressed as:

$$b_{m,-n} = \sum_{l=-\infty}^{+\infty} e^{-\frac{[-nC_1-(n+mK)C_2+lC_1]^2}{2}} \times e^{-\frac{[-(n+mK)(C_2T_1+B_4)+B_2mK]^2}{2}} \times J_m[(n+mK)(A_2B_2-A_2B_4)-lB_2A_2] \times J_l[(n+mK)B_4A_3] \times J_{n-l}[-\alpha(B_1+B_4)A_1] + mK(B_1+B_2)A_1+lB_1A_1 \quad (9)$$

SIMULATION

Table 1: Main Beam Parameters in Simulation

Parameter	Value
Energy	2 GeV
Energy spread	0.1 %
Peak current	100 A
Geometric horizontal emittance	1 nm rad
Geometric vertical emittance	10 pm rad
Vertical beta function	250 m

The evolution of the beam longitudinal phase space is shown in Fig. 1. To better demonstrate the physics process behind the proposed scheme, we assume that the three lasers in the modulators have the same wavelength. The parameters used here are: $T_1 = 100$, $A_1 = A_3 = 1$, $C_1 = 0.00992$, $B_1 = -1$, $A_2 = 0.02$, $B_2 = -B_3 = 14.17$, $C_2 = -2.126 \times 10^{-4}$, and $B_4 = 1.25$.

The microbunching induced by the ADM mechanism is shown in Fig. 1 (a). Then the beam will pass through the first chicane with $B_2 = 14.17$. Similar to the EEHG scheme, the energy bands are generated as shown in Fig. 1 (b). The energy spread of these bands are small. When the beam go through the second modulator and interact with the second seed laser, the beam phase space evolves to Fig. 1 (c). Due to the low energy modulation amplitude induced by the second seed laser in the second modulator, it is hard to see the difference between Figs. 1 (b) and 1 (c). After that, the beam will pass through the second chicane with $B_3 = -14.17$, which will amplify the modulation imprinted in the second modulator and we can find the fine structure, as shown in Fig. 1 (d). The third laser in the third modulator gives the beam the same energy modulation amplitude as that in the first modulator, but with a π phase shift. The phase space at the exit of the third modulator is shown in Fig. 1 (e). Finally, the beam will pass through the dogleg to convert the energy modulation into density modulation, as shown in Fig. 1 (f).

Next, we will show how to generate the coherent harmonic radiation with the proposed scheme. As an example, we assume that the seed lasers in the first and third modulator have the same wavelength of 266 nm. The seed laser in the

second modulator have the wavelength of 26.6 nm. High harmonic generation (HHG) source with low power can meet the demand in the proposed scheme.

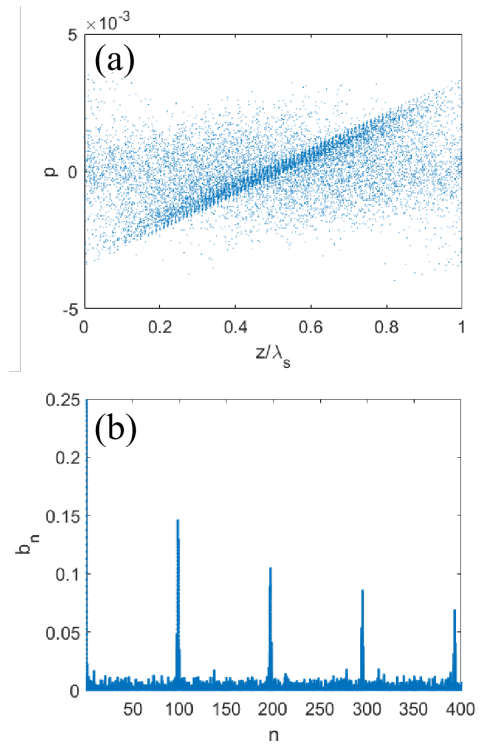


Figure 2: Bunching factor at 0.9 nm for various B_3 and B_4 (a); A_2 and A_3 (b).

For $T_1 = 100$, $A_1 = -A_3 = 1$, $C_1 = 0.00992$, $B_1 = 1$, $B_2 = -B_3 = 9.448$, $A_2 = 0.02$, $C_2 = -7.09 \times 10^{-5}$, and $B_4 = 0.968$, the beam longitudinal phase space at the exit of the second dogleg is shown in Fig. 2(a). According to the beam distribution in Fig. 2(a), the bunching factor at 0.9 nm (295th harmonic number) is about 8.4%, as shown in Fig. 2(b). The bunching factor is large enough to generate the fully coherent radiation at 0.9 nm in the following radiator.

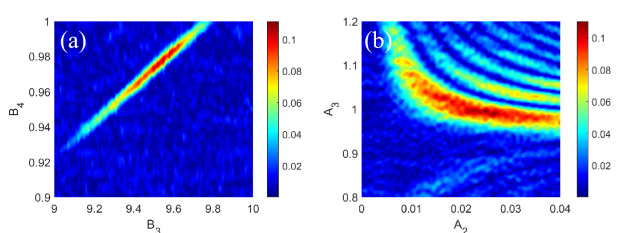


Figure 3: Bunching factor at 0.9 nm for various B_3 and B_4 (a); A_2 and A_3 (b).

To study the stability of our proposed scheme, we performed a parameter scan for A_2 , A_3 , B_3 and B_4 around their optimized parameters, while keeping the other parameters at the regular values. As shown in Fig. 3 (a), the fluctuation of the chicane strength should be controlled within 2% to produce a large bunching factor at a given harmonic number. Figure 3 (b) shows that the bunching is more sensitive

to A_3 than A_2 which reduces the burden of the stability of HHG seed. The power fluctuation of the laser in the third modulator should be kept within 4% to maintain the large bunching factor.

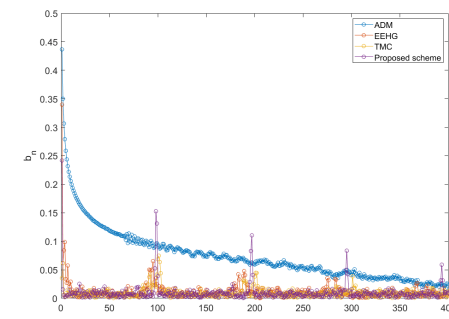


Figure 4: Bunching factor at the various harmonic number for ADM, EEHG, TMC and proposed schemes.

Table 2: Energy modulation amplitude used in several schemes

	A_1	A_2	A_3
ADM	10	×	×
EEHG	10	10	×
TMC	11	0.05	11
Proposed scheme	1	0.02 (26.6 nm)	-1

Finally, we compared the proposed scheme with other different harmonic generation schemes. The bunching factor at the various harmonic number for the proposed scheme and other conventional schemes are shown in Fig. 4. The energy modulation amplitude used in these schemes are summarized in Table 2. As we can see in Fig. 4, the proposed scheme has the maximum bunching factor at the high harmonic (like the 300th harmonic). This is because the proposed scheme combines the advantage of other schemes. The complex scheme is easier to get high bunching factor at the high harmonic number through controlling more variables.

CONCLUSION

In this paper, we proposed a novel scheme based on ADM mechanism for generating high harmonic in the storage ring. It has potential to produce the fully coherent radiation at the sub-nanometer wavelength in the storage ring. Besides, we also analyzed the fluctuation of the parameters in the proposed scheme. Finally, we compared the proposed scheme with other conventional schemes.

REFERENCES

- [1] G. Geloni, V. Kocharyan, and E. Saldin, "A novel self-seeding scheme for hard x-ray fels," *Journal of Modern Optics*, vol. 58, no. 16, pp. 1391–1403, 2011, doi:10.1080/09500340.2011.586473

[2] J. Amann *et al.*, "Demonstration of self-seeding in a hard x-ray free-electron laser," *Nature Photonics*, vol. 6, no. 10, pp. 693–698, 2012, doi: 10.1038/nphoton.2012.180

[3] K.-J. Kim and Y. V. Shvyd'ko, "Tunable optical cavity for an x-ray free-electron-laser oscillator," *Physical Review Special Topics-Accelerators and Beams*, vol. 12, no. 3, p. 030703, 2009, doi: 10.1103/PhysRevSTAB.12.030703

[4] K. Li and H. Deng, "Systematic design and three-dimensional simulation of x-ray fel oscillator for shanghai coherent light facility," *Nuclear Instruments and Methods in Physics Research Section A: Accelerators, Spectrometers, Detectors and Associated Equipment*, vol. 895, pp. 40–47, 2018, doi: 10.1016/j.nima.2018.03.072

[5] M. Opronolla *et al.*, "High repetition rate and coherent free-electron laser oscillator in the tender x-ray range tailored for linear spectroscopy," *Applied Sciences*, vol. 11, no. 13, p. 5892, 2021, doi: 10.3390/app11135892

[6] D. Xiang and G. Stupakov, "Echo-enabled harmonic generation free electron laser," *Physical Review Special Topics-Accelerators and Beams*, vol. 12, no. 3, p. 030702, 2009, doi: 10.1103/PhysRevSTAB.12.030702

[7] C. Feng and Z. Zhao, "A storage ring based free-electron laser for generating ultrashort coherent euv and x-ray radiation," *Scientific reports*, vol. 7, no. 1, p. 4724, 2017, doi: 10.1038/s41598-017-04962-5

[8] D. Xiang and G. Stupakov, "Triple modulator–chicane scheme for seeding sub-nanometer x-ray free-electron lasers," *New Journal of Physics*, vol. 13, no. 9, p. 093028, 2011, doi: 10.1088/1367-2630/13/9/093028